$ZnGa_2O_4:Cr^{3+}$: a new red long-lasting phosphor with high brightness

Aurélie Bessière,[1,2,*] Sylvaine Jacquart,[1,2] Kaustubh Priolkar,[2] Aurélie Lecointre,[1] Bruno Viana,[1] and Didier Gourier[1]

[1]*Chimie Paristech, Laboratoire de Chimie Matière Condensée de Paris, UPMC, Collège de France, UMR - CNRS 7574, 11 rue Pierre et Marie Curie, 75231 Paris Cedex 05, France*
[2]*Department of Physics, Goa University, Taleigao Plateau, Goa 403206, India*
**aurelie-bessiere@chimie-paristech.fr*

Abstract: $ZnGa_2O_4:Cr^{3+}$ is shown to be a new bright red UV excited long-lasting phosphor potentially suitable for *in vivo* imaging due to its 650 nm-750 nm emission range. Photoluminescence and X-ray excited radioluminescence show the $^2E \rightarrow {}^4A_2$ emission lines of both ideal Cr^{3+} and Cr^{3+} distorted by a neighboring antisite defect while long-lasting phosphorescence (LLP) and thermally stimulated luminescence (TSL) almost exclusively occur via distorted Cr^{3+}. The most intense LLP is obtained with a nominal Zn deficiency and is related to a TSL peak at 335K. A mechanism for LLP and TSL is proposed, whereby the antisite defect responsible for the distortion at Cr^{3+} acts as a deep trap.

OCIS codes: (160.2540) Fluorescent and luminescent materials; (160.2900) Optical storage materials; (160.4670) Optical materials; (160.4760) Optical properties; (160.6990) Transition-metal-doped materials; (300.6250) Spectroscopy, condensed matter.

References and links

1. V. Ntziachristos, "Fluorescence molecular imaging," Annu. Rev. Biomed. Eng. **8**(1), 1–33 (2006).
2. Q. le Masne de Chermont, C. Chanéac, J. Seguin, F. Pellé, S. Maîtrejean, J. P. Jolivet, D. Gourier, M. Bessodes, and D. Scherman, "Nanoprobes with near-infrared persistent luminescence for *in vivo* imaging," Proc. Natl. Acad. Sci. U.S.A. **104**(22), 9266–9271 (2007).
3. R. Weissleder and V. Ntziachristos, "Shedding light onto live molecular targets," Nat. Med. **9**(1), 123–128 (2003).
4. Q. le Masne de Chermont, D. Scherman, M. Bessodes, F. Pellé, S. Maitrejean, J-P. Jolivet, C. Chanéac, D. Gourier, "Nanoparticules à luminescence persistante pour leur utilisation en tant qu'agent de diagnostique destiné à l'imagerie optique in vivo," CNRS patent, internat. ext. WOEP06067950, WO2007048856, 30/10/2006.
5. I. J. Hsieh, K. T. Chu, C. F. Yu, and M. S. Feng, "Cathodoluminescent characteristics of $ZnGa_2O_4$ phosphor grown by radio frequency magnetron sputtering," J. Appl. Phys. **76**(6), 3735–3739 (1994).
6. I. K. Jeong, H. L. Park, and S. Mho, "Two self-activated optical centers of blue emission in zinc gallate," Solid State Commun. **105**(3), 179–183 (1998).
7. S. Itoh, H. Toki, Y. Sato, K. Morimoto, and T. Kishino, "The $ZnGa_2O_4$ phosphor for low-voltage blue cathodoluminescence," J. Electrochem. Soc. **138**(5), 1509–1512 (1991).
8. L. E. Shea, R. K. Datta, and J. J. Brown, "Photoluminescence of Mn^{2+}-activated $ZnGa_2O_4$," J. Electrochem. Soc. **141**(7), 1950–1954 (1994).
9. P. Dhak, U. K. Gayen, S. Mishra, P. Pramanik, and A. Roy, "Optical emission spectra of chromium doped nanocrystalline zinc gallate," J. Appl. Phys. **106**(6), 063721 (2009).
10. D. Errandonea, R. S. Kumar, F. J. Manjón, V. V. Ursaki, and E. V. Rusu, "Post-spinel transformations and equation of state in $ZnGa_2O_4$: Determination at high pressure by in situ x-ray diffraction," Phys. Rev. B **79**(2), 024103 (2009).
11. R. D. Shannon and C. T. Prewitt, "Effective ionic radii in oxides and fluorides," Acta Crystallogr. B **25**(5), 925–946 (1969).
12. H. M. Kahan and R. M. Macfarlane, "Optical and microwave spectra of Cr^{3+} in the spinel $ZnGa_2O_4$," J. Chem. Phys. **54**(12), 5197–5205 (1971).
13. W. Zhang, J. Zhang, Z. Chen, T. Wang, and S. Zheng, "Spectrum designation and effect of Al substitution on the luminescence of Cr^{3+} doped $ZnGa_2O_4$ nano-sized phosphors," J. Lumin. **130**(10), 1738–1743 (2010).
14. W. Mikenda and A. Preisinger, "N-lines in the luminescence spectra of Cr^{3+}-doped spinels: I. Identification of N-lines," J. Lumin. **26**(1-2), 53–66 (1981).

#144041 - $15.00 USD Received 16 Mar 2011; revised 28 Apr 2011; accepted 5 May 2011; published 9 May 2011

15. W. Mikenda and A. Preisinger, "N-lines in the luminescence spectra of Cr^{3+}-doped spinels: III. Origins of N-lines," J. Lumin. **26**(1-2), 67–83 (1981).
16. W. Mikenda, "N-lines in the luminescence spectra of Cr^{3+}-doped spinels: III. Partial spectra," J. Lumin. **26**(1-2), 85–98 (1983).
17. J. Derkosch and W. Mikenda, "N-lines in the luminescence spectra of Cr^{3+}-doped spinels: IV. Excitation spectra," J. Lumin. **28**(4), 431–441 (1981).
18. W. Nie, F. M. Michel-Calendini, C. Linares, G. Boulon, and C. Daul, "New results on optical properties and term-energy calculations in Cr^{3+}-doped $ZnAl_2O_4$," J. Lumin. **46**(3), 177–190 (1990).
19. R. Hill, J. Craig, and G. V. Gibbs, "Systematics of the spinel structure type," Phys. Chem. Miner. **4**(4), 317–339 (1979).
20. G. Anoop, K. Mini Krishna, and M. K. Jayaraj, "Influence of a dopant source on the structural and optical properties of Mn doped $ZnGa_2O_4$ thin films," Appl. Phys., A Mater. Sci. Process. **90**(4), 711–715 (2008).
21. A. Lecointre, B. Viana, Q. LeMasne, A. Bessière, C. Chanéac, and D. Gourier, "Red long-lasting luminescence in Clinoenstatite," J. Lumin. **129**(12), 1527–1530 (2009).
22. A. Lecointre, A. Bessière, B. Viana, R. Aït Benhamou, and D. Gourier, "Thermally stimulated luminescence of $Ca_3(PO_4)_2$ and $Ca_9Ln(PO_4)_7$ (Ln = Pr, Eu, Tb, Dy, Ho, Er, Lu)," Radiat. Meas. **45**(3-6), 273–276 (2010).
23. A. Lecointre, A. Bessière, B. Viana, and D. Gourier, "Red persistent luminescent silicate nanoparticles," Radiat. Meas. **45**(3-6), 497–499 (2010).
24. A. Lecointre, A. Bessière, A. J. J. Bos, P. Dorenbos, B. Viana, and S. Jacquart, "Designing a red persistent luminescence phosphor: the example of $YPO_4:Pr^{3+},Ln^{3+}$ (Ln = Nd, Er, Ho, Dy)," J. Phys. Chem. C **115**(10), 4217–4227 (2011).
25. K. Uheda, T. Maruyama, H. Takisawa, and T. Endo, "Synthesis and long-period phosphorescence of $ZnGa_2O_4$: Mn^{2+} spinel," J. Alloy. Comp. **262–263**, 60–64 (1997).

1. Introduction

Use of luminescent systems for *in vivo* imaging is of great interest to investigate pathologies in animal models [1]. Such non-invasive visualization tools offer great advantages in terms of cost and simplicity over expensive techniques at the laboratory scale like micro-Positron Emission Tomography or micro-Magnetic Resonance Imaging. It was recently shown that optical imaging could be advantageously carried out by using as luminescent probe a persistent phosphor emitting in the red/near-infrared part of the spectrum [2]. A red/near-infrared emission is necessary for luminescence to pass through the animal tissues since the main components of the tissues strongly absorb ultraviolet (UV)-blue-green and far-infrared parts of the spectrum [3]. By using persistent luminescence nanoparticle the illumination of the animal becomes unnecessary and autofluorescence of the tissues is avoided. UV excitation of the particle is carried out before its injection and therefore is not attenuated by the tissues. The technique was first demonstrated in 2007 with $Ca_{0.2}Zn_{0.9}Mg_{0.9}Si_2O_6:Eu^{2+},Dy^{3+},Mn^{2+}$ (CZMSO) nanoparticles, from which persistent luminescence was detected in a small animal vasculature for up to one hour after their injection [2,4].

In this context we report here on a new red long-lasting phosphorescence (LLP) material potentially suitable for *in vivo* imaging. $ZnGa_2O_4$ is a wide band gap semiconductor which allows doping by luminescent ions such as transition metal ions. Due to its excellent chemical and thermal stability it has been considered as a phosphor of choice for plasma and field emission displays [5]. $ZnGa_2O_4$ shows blue luminescence attributed to self-activated centres when undoped [6,7], intense green emission when doped with Mn^{2+} [8] and red luminescence with Cr^{3+} doping [9]. It crystallizes in the normal spinel structure (space group O_h^7 (Fd3m)) with Zn^{2+} ions occupying tetrahedral sites (T_d) and Ga^{3+} ions occupying octahedral sites (D_{3d}) [10]. $ZnGa_2O_4$ is an ideal host lattice for Cr^{3+} since the latter presents an ionic radius of 0.62 Å identical to the one of Ga^{3+} in octahedral coordination [11]. When excited, Cr^{3+} emits *via* its $^2E \rightarrow {}^4A_2$ transition which gives rise to a far red luminescence with a maximum at 696 nm in the zinc gallate host [9,12]. This wavelength range is totally suitable for *in vivo* imaging as it corresponds to a transmission maximum for the biological tissues [3].

In this paper we show that $ZnGa_2O_4:Cr^{3+}$ powder compares better than CZMSO used up to now for *in vivo* imaging with UV excitation [2]. Mechanism of LLP is investigated by varying the nominal Zn/Ga stoichiometry and by using UV and X-ray excitation to record wavelength-resolved persistent luminescence and thermally stimulated luminescence (TSL).

#144041 - $15.00 USD Received 16 Mar 2011; revised 28 Apr 2011; accepted 5 May 2011; published 9 May 2011

2. Experimental

The $ZnGa_2O_4$:Cr powders were synthesized by a solid state method. Ga_2O_3 powder (Aldrich 99,99 + %), ZnO powder (Loba-Chemie GR 99%) and CrO_3 red flakes (Sisco Research Laboratory AR 99% min.) were mixed in an agate mortar with propan-2-ol. Pellets were prepared from the powder mixtures and fired in air at 1300°C for 6h. All the compounds were nominally doped with 0.5% mol chromium relative to gallium. Three compounds were prepared with various Zn/Ga stoichiometry, their nominal compositions being $Zn_{0.99}Ga_{1.99}Cr_{0.01}O_4$ (Zn-deficient compound, noted Zn-d) $ZnGa_{1.99}Cr_{0.01}O_4$ (stoichiometric compound, noted Zn-s) and $Zn_{1.01}Ga_{1.99}Cr_{0.01}O_4$ (Zn-excess compound, noted Zn-e) respectively. X-ray diffraction of the three compounds evidenced pure $ZnGa_2O_4$ crystalline phase with cubic spinel structure (not shown here).

Photoluminescence (PL) spectra were measured at room temperature (RT) on powder pellets with a Varian Cary Eclipse spectrofluorimeter. X-ray excited radioluminescence (XRL), LLP and TSL measurements were run on 1 mm-thick pellets of the powdered samples. For all three experiments light is collected *via* an optical fiber by a Scientific Pixis 100 CCD camera cooled at −65°C coupled with an Acton SpectraPro 2150i spectrometer for spectral analysis. X-ray excitation is produced by a molybdenum tube operated at 50 kV and 20 mA. UV excitation is produced by a 350 W xenon lamp filtered with a FG UV11 filter to remove visible excitation (bandpass 250-380 nm). In TSL experiments the 1 mm-thick pellet is fixed with a silver glue on the cold finger of a closed cycle helium cryogenerator. UV irradiation is performed at 30 K through a quartz window of the cryostat at 45° angle from the pellet surface and luminescence is detected through a different quartz window at 45° angle from the pellet surface. A heating rate of 10 K/min is applied. Prior to all LLP and TSL experiments the samples were bleached for 20 minutes at 200°C and kept in the dark before the experiment.

3. Results and discussion

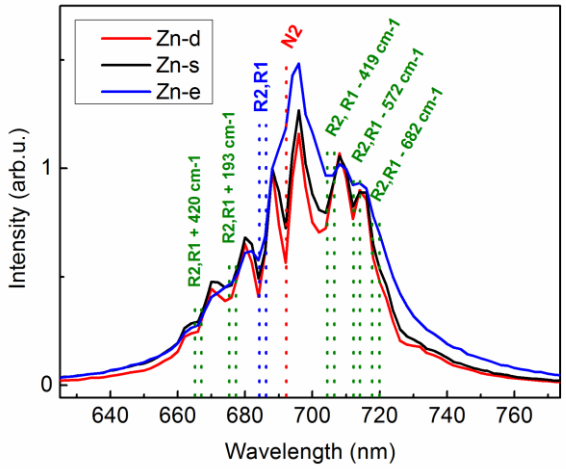

Fig. 1. PL spectra excited at 247 nm of Zn-d, Zn-s and Zn-e $ZnGa_2O_4$:Cr^{3+} compounds. Dotted lines show the attribution of Cr^{3+} lines in $ZnGa_2O_4$:Cr^{3+} at 13K according to Zhang *et al.* [13].

Figure 1 shows the PL spectra of the Cr^{3+}-doped $ZnGa_2O_4$ powders. The spectra display several narrow lines that constitute recognizable features of Cr^{3+} ion emission in a strong field with octahedral coordination. PL features of $ZnGa_2O_4$:Cr^{3+} at 13K as reported by Zhang *et al.* [13] are shown in Fig. 1 as dotted lines. At 13K, these authors report two zero phonon (ZP) lines known as R2 and R1 for the $^2E \rightarrow {}^4A_2$ transition of Cr^{3+}. A weak trigonal distortion

#144041 - $15.00 USD Received 16 Mar 2011; revised 28 Apr 2011; accepted 5 May 2011; published 9 May 2011

around Cr^{3+} splits the ^2E level into ^2E ($\bar{E}$) and ^2E ($2\bar{A}$) separated by 40 cm^{-1} [12] giving rise to the two R lines. R2 and R1 have also been observed at 300K by Kahan *et al.* [12] with a high-resolution set-up at 14556 cm^{-1} (687.0 nm) and 14518.8 cm^{-1} (688.8 nm), respectively. Their position is in total agreement with the feature here observed at 688 nm which we attribute to the unresolved (R2,R1) doublet since our set-up does not allow resolution of these two lines. Since all lines should be red-shifted from 13K (Zhang *et al.* [12]) to RT (our experiment), the phonon side bands (PSB) of the R lines were identified in the spectra of Fig. 1 at 708 nm, 715 nm and 722 nm for the Stokes PSB and at 670 nm and 680 nm for the Anti-Stokes PSB. The PSB positions are consistent with data from infrared and Raman spectroscopies [13].

An additional line observed at 695 nm in Fig. 1 is not accounted for by the above mentioned transitions. It therefore originates from another type of Cr^{3+} ion with perturbed short-range crystalline order relative to the ideal octahedral coordination of the normal spinel. The feature was here observed at 695 nm, i.e. at 147 cm^{-1} lower energy than the (R2,R1) doublet. According to Mikenda *et al.* [14] a structure-dependent line named N2 for Cr^{3+} in $ZnGa_2O_4$ lies at 134 cm^{-1} lower energy than R1. We therefore attribute the 695 nm line to the N2 line of Cr^{3+}. After extensive investigation, particularly by Mikenda *et al.* [15–17] and Nie *et al.* [18], the N2 line of Cr^{3+} in $ZnGa_2O_4$ spinel was established to originate from Cr^{3+} ions possessing an environment distorted by an antisite defect, located in the first cationic neighbors of Cr^{3+}. Our chromium-doped zinc gallates therefore present two types of doping ions: (i) Cr^{3+} in an ideal normal spinel environment noted Cr_n^{3+} and (ii) Cr^{3+} in a slightly distorted environment noted Cr_{dis}^{3+}. $ZnGa_2O_4$ is known to crystallize in an almost normal spinel structure with a few percent inversion [19]. The inversion percentage varies with synthesis conditions and is favored by high temperature synthesis [6,20]. The comparison of the three compounds spectra shows that the intensity of the N2 line relative to the R lines increases as the stoichiometry evolves from a nominal zinc deficiency towards a zinc excess. More antisite defects seem therefore present as the Zn/Ga nominal ratio is increased. Considering the two possible antisite defects of opposite charge that can distort the coordination polyhedron of Cr^{3+}, namely Zn_{Ga}' (negatively charged) and Ga_{Zn}° (positively charged), the position of the N2 line at a photon energy 147 cm^{-1} below the (R1,R2) line of undistorted Cr_n^{3+} indicates that the crystal field is smaller for Cr_{dis}^{3+} than for Cr_n^{3+}. This suggests that the neighboring defect is positively charged, as is a Ga^{3+} ion in Zn^{2+} site (Ga_{Zn}°).

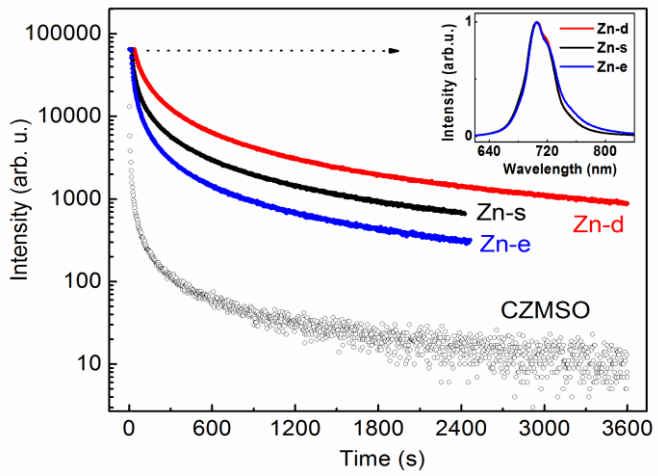

Fig. 2. LLP decays of Zn-d, Zn-s and Zn-e $ZnGa_2O_4$:Cr^{3+} compounds at 705 nm and of the silicate reference at 695 nm recorded at 303 K after 5 minutes UV excitation. Inset: normalized LLP spectra of $ZnGa_2O_4$:Cr^{3+} compounds 45 s after the end of the excitation.

#144041 - $15.00 USD Received 16 Mar 2011; revised 28 Apr 2011; accepted 5 May 2011; published 9 May 2011

LLP was measured after UV excitation to compare the Cr^{3+}-doped zinc gallates to the phosphor previously used for the demonstration of imaging (referred to as CZMSO). This reference phosphor is a silicate of nominal formula $Ca_{0.2}Zn_{0.9}Mg_{0.9}Si_2O_6:Eu^{2+},Mn^{2+},Dy^{3+}$ described in [2]. Both phosphors were excited for 5 minutes with a filtered xenon lamp before their LLP was recorded for up to one hour at an ambient temperature of 30°C. The normalized LLP spectra of the $ZnGa_2O_4:Cr^{3+}$ compounds recorded 45 s after the end of the excitation are shown in the inset of Fig. 2. Due to wide monochromator slits the spectra do not show as resolved lines as in Fig. 1 but they still display the $^2E \rightarrow {}^4A_2$ luminescence of Cr^{3+}. LLP decays at the wavelength of emission maximum are compared in the main plot of Fig. 2. The Cr^{3+}-doped zinc gallates showed a highly enhanced intensity relative to CZMSO. As its emission lies in the highest transmission spectral range of the biological tissues, $ZnGa_2O_4:Cr^{3+}$ is an excellent new candidate for LLP imaging. Amongst the three $ZnGa_2O_4:Cr^{3+}$ materials more intense LLP was obtained as the compound is nominally more Zn-deficient.

The compound with the most intense LLP, i.e. Zn-d, was investigated further. Both immediate and delayed (i.e. "persistent" or "long-lasting") luminescence spectra of Zn-d were recorded under X-ray excitation. The $ZnGa_2O_4:Cr^{3+}$ pellet was excited by X-rays for two minutes. During this time an XRL spectrum was recorded and is presented in Fig. 3. After two minutes, X-ray irradiation was switched off and an X-ray induced long-lasting phosphorescence (XLLP) spectrum was recorded 20 seconds after the excitation had ended. The XRL spectrum displayed the same lines as shown in the PL spectrum of Fig. 1. An intense XLLP was observed when the excitation is switched off, and its normalized spectrum shown in Fig. 3 appeared very different from the XRL spectrum, as the N2 line was then highly predominant. One can distinguish the weak PSB identified above as the PSB of the R lines. The emission spectrum of Cr_n^{3+} is therefore still present but with a strongly reduced intensity. The striking difference between the XRL and the XLLP spectra confirms the existence of two distinct types of Cr^{3+} ions in the gallate. Undistorted Cr_n^{3+} shows very little XLLP whereas Cr_{dis}^{3+} is related to an intense delayed emission. Note that in the XRL spectrum the PSB of the R lines appear quite intense relative to the ZP lines. This is expected for a centrosymmetric environment around undistorted Cr_n^{3+}. Purely electronic transitions (R lines) remain forbidden relative to phonon coupling transitions in a centrosymmetric environment. On the contrary the PSB of the N2 line are expected to present a smaller intensity relative to the ZP line since the symmetry of the crystal field is distorted by a closeby antisite defect. This is why the N2 ZP line appears very distinct in the XLLP spectrum.

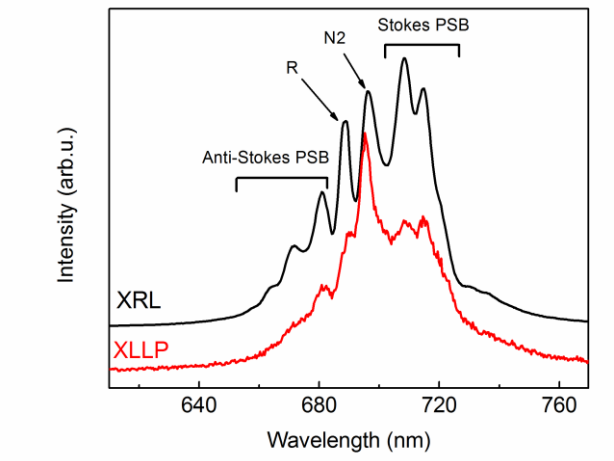

Fig. 3. XRL and XLLP spectra of Zn-d $ZnGa_2O_4:Cr^{3+}$ at 293 K.

#144041 - $15.00 USD Received 16 Mar 2011; revised 28 Apr 2011; accepted 5 May 2011; published 9 May 2011

TSL of Zn-d was measured after 5 minutes UV irradiation by the filtered xenon lamp at 30K. The glow curve for the emission at 694 nm is shown in Fig. 4(a). The spectra at selected points of the glow curves (A, B, C and D) are displayed in Fig. 4(b). Decaying intensity right at the beginning of the glow curve (point A) reflects a possible athermal tunnelling recombination process, weak in intensity relative to the thermally stimulated processes. However it is interesting to compare the shape of the spectrum at position A with spectra at positions B, C and D (see Fig. 4(b)). At point A, the spectrum was clearly composed of the (R2,R1) lines at 688 nm and of the N2 line at 694 nm similarly to the XRL spectrum presented in Fig. 3. The spectra only differed in terms of PSB since at 30K the Stokes PSB were present whereas, as expected at low temperature, no anti-Stokes PSB were observed. On the contrary the spectra at points B, C, and D (maxima of the TSL glow curve) displayed very much enhanced N2 line relative to the R and PSB lines as already observed in the XLLP spectrum of Fig. 3. This shows two different behaviors in terms of emitting ions and charge trapping and release in the material. On the one hand a minor part of the electrons and holes created by UV excitation get weakly trapped and then recombine *via* a tunnelling mechanism that leads to luminescence of all types of Cr^{3+} ions. On the other hand and more interestingly, Cr_{dis}^{3+} is the main emitting centre for TSL peaks B, C and D, which indicates that it is directly involved in the recombination process. Let us note that no difference but the effect of temperature on the PSB could be noticed from the comparison of spectra at points B, C and D. Hence the same defect spatially related to Cr_{dis}^{3+} is at stake in B, C and D, i.e. all along the TSL glow curve.

As the TSL was recorded at a slow heating rate (10 K/min.) the LLP observed at RT is mainly related to peak D of the glow curve, while peaks B and C should only contribute to the initial decay of the LLP curve. For a short period of time the slitwidths of the monochromator were suddenly reduced to the minimum at 318K in the rise of peak D showing the spectrum presented in the inset of Fig. 4(a). Again the spectrum showed a clear predominance of the N2 line of Cr_{dis}^{3+} and is totally similar to the XLLP spectrum shown in Fig. 3. Therefore the mechanism of the LLP is the same whatever the excitation source (UV or X-rays).

From the above results and due to the property of Cr^{3+} to constitute a very sensitive local probe, we can propose a possible mechanism for the LLP in $ZnGa_2O_4:Cr^{3+}$. Previous works showed that antisite defects of the type $Ga_{Zn}°$ and Zn_{Ga}' are present in the compound [6,19]. Further because ZnO is known to evaporate at lower temperature than Ga_2O_3 and because the compounds were synthesized at 1300°C it is reasonable to assume that Zn vacancies, noted as V_{Zn}'' are also present. The fact that both LLP and TSL are mainly due to Cr_{dis}^{3+} indicates that this species is a recombination centre. It is thus tempting to assign the nearby antisite defect to a trap. Following our hypothesis that the latter is a $Ga_{Zn}°$ defect (which we note $Ga_{Zn}°\{Cr^{3+}\}$), one may propose a mechanism explaining the dominant contribution of Cr_{dis}^{3+} to LLP and TSL. The UV irradiation creates electrons (e') and holes (h°) that are trapped by defects. Electrons are trapped around Cr_{dis}^{3+} ions according to the reaction: $Ga_{Zn}°\{Cr^{3+}\} + e' \rightarrow Ga_{Zn}^{x}\{Cr^{3+}\}$, while holes are trapped at negatively charged defect sites such as Zn_{Ga}' or V_{Zn}''. Holes released from these traps by thermal activation then recombine at Cr_{dis}^{3+} site, giving the N2 emission line according to the reaction: $Ga_{Zn}^{x}\{Cr^{3+}\} + h° \rightarrow [Ga_{Zn}°\{Cr^{3+}\}]^* \rightarrow Ga_{Zn}°\{(Cr^{3+})^*\} \rightarrow Ga_{Zn}°\{Cr^{3+}\} + h\nu$ where * represents excited states.

With the comparison of the three samples with different Zn/Ga ratio we found that more antisite defects were present close to Cr^{3+} with increasing Zn/Ga ratio, whereas the LLP was more intense with decreasing Zn/Ga ratio. Decreasing the Zn/Ga ratio favors more Zn vacancies (and thus more hole traps) which may then be responsible for the enhanced LLP. Within this hypothesis the TSL peak D as well as the LLP at RT are due to V_{Zn}'' from which

#144041 - $15.00 USD Received 16 Mar 2011; revised 28 Apr 2011; accepted 5 May 2011; published 9 May 2011

the holes get thermally detrapped to recombine at Cr_{dis}^{3+} site. Further experiments will be carried out in the future to constrain the proposed mechanism.

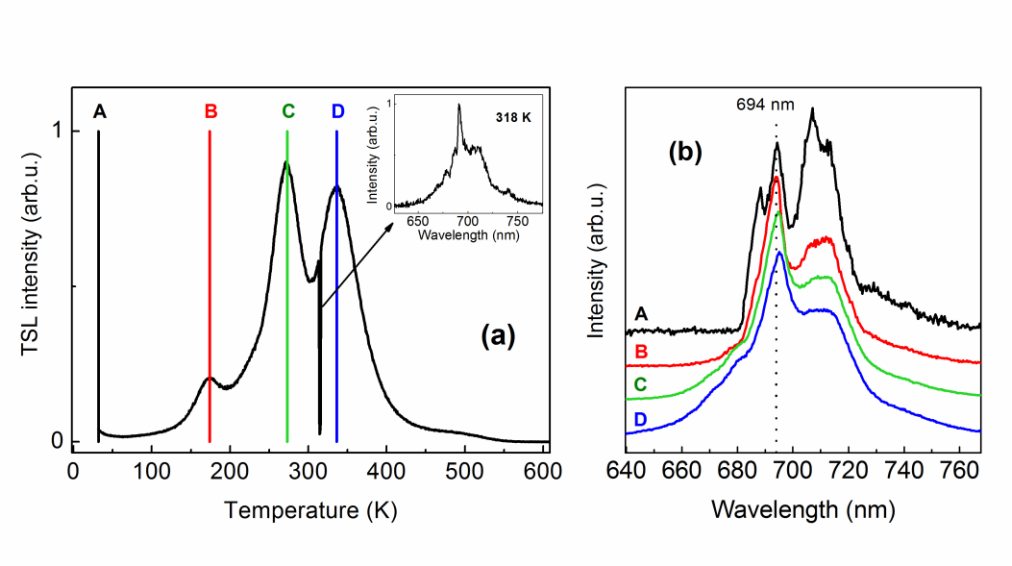

Fig. 4. (a) TSL of Zn-d $ZnGa_2O_4:Cr^{3+}$ at 694 nm after 5 minutes UV excitation. Inset: TSL spectrum at 318 K with reduced slitwidths. (b) TSL spectra at the beginning of the TSL curve (A) and at the main TSL peak maxima (B, C and D).

4. Conclusion

We showed in this work that $ZnGa_2O_4:Cr^{3+}$ is a new high-performance red long-lasting phosphor, compared to CZMSO used for demonstrating the technique of LLP *in vivo* imaging [2]. On the contrary to other red LLP materials studied for this application [21–24] $ZnGa_2O_4:Cr^{3+}$ could be conveniently excited through its bandgap by UV light. After 5 minutes excitation it emitted light around 695 nm via the $^2E \rightarrow {}^4A_2$ transition of Cr^{3+} for a prolonged time. This emission range perfectly matched the optical window of biological tissues and as such may be readily detected across small animal tissues.

In addition to the exciting properties of $ZnGa_2O_4:Cr^{3+}$ for imaging, the compound revealed new elements in the field of LLP. Firstly $ZnGa_2O_4$ may be an intrinsic persistent phosphor since intense green [25] and now red LLP were observed in the same host. Furthermore no codoping was necessary to obtain intense persistent luminescence which makes investigation of mechanisms easier and decreases the chances of non-radiative loss. The use of a small dopant concentration (0.5%) and of a similar size dopant as the substituted ion (the ionic radii of Cr^{3+} and Ga^{3+} are identical) also reduces the occurrence of defects that constitute potential loss centres. Secondly the use of Cr^{3+} as both luminescent centre and probe of the local environment appeared as of uttermost use in the investigation of the mechanisms. The very narrow emission lines of Cr^{3+} ions in Ga^{3+} sites are so sensitive to chromium environment that the coordination sphere of the luminescent centre Cr^{3+} can be elucidated. Hence we showed that antisite defects Ga_{Zn} of the $ZnGa_2O_4$ spinel structure were likely to be involved in the charge trapping and recombination processes responsible for LLP in $ZnGa_2O_4:Cr^{3+}$. The LLP intensity was singularly improved by decreasing the nominal Zn/Ga ratio, i.e. probably by creating more Zn vacancies that constitute the thermally emptied traps in the LLP mechanism.

#144041 - $15.00 USD Received 16 Mar 2011; revised 28 Apr 2011; accepted 5 May 2011; published 9 May 2011